Frequency-Domain Analysis of a Mixer-First Receiver Using Conversion Matrices

Sameed Hameed*, Mansour Rachid†, Babak Daneshrad* and Sudhakar Pamarti*
Email: {sameed, babak, spamarti}@seas.ucla.edu mansour@silvustechnologies.com
*Electrical Engineering Department, University of California, Los Angeles, CA, USA
†Silvus Technologies, Inc., Los Angeles, CA, USA

***Abstract*—The analysis of a mixer-first receiver using conversion matrices is presented. Conversion matrices provide a systematic approach to analyze linear periodically time-varying (LPTV) circuits. Using conversion matrices of LPTV components in a frequency domain equivalent circuit allows analysis similar to a linear time invariant (LTI) circuit. For example, Ohm's law, Kirchhoff's voltage and current laws, impedance combination rules, etc., can all be used in such equivalent circuits. On applying this method to a mixer-first receiver, a common LPTV circuit, results already established in prior art are reproduced accurately. Further, effects of a few important non-idealities, such as clock overlaps, imperfect clock edges and parasitic components that were not considered previously, are also calculated and verified.**

I. Introduction

Advances in circuit techniques such as N-path filters and mixer-first receivers [4], [5], [9] are enabling programmable receivers necessary for software-defined radios (SDRs) and cognitive radios (CRs) [1], [2]. Analysis of such circuits, which are from a class of circuits known as "linear periodically time-varying" (LPTV) circuits, however, poses a formidable challenge. Generally, the presence of clock-driven switching elements leads to frequency translation of the circuit's voltages and currents, and so traditional Laplace or Fourier domain linear time invariant (LTI) circuit analysis techniques have limited applicability.

Several techniques to analyze LPTV circuits have been reported. The behaviour of any LPTV system in the freqeuncy domain can be shown to follow:

$$Y(\omega) = \sum_{m=-\infty}^{\infty} H_m(\omega) U(\omega - m\omega_p), \tag{1}$$

where $U(\omega)$ and $Y(\omega)$ are the Fourier transforms of the input and output respectively of an LPTV system with a fundamental period $2\pi/\omega_p$, and the determination of the set of functions, $H_m(\omega)$, known as "*harmonic transfer functions*" (HTFs), becomes the goal [3]-[11]. Analogously in LTI systems only a single function, $H_0(\omega)$, which is the transfer function, is required. Several works derive the HTFs by applying circuit laws in the time domain and then applying a Fourier transform [4], [5]. State-space-based approaches, which treat the circuit as periodically moving through a set of states, have also been shown to be useful [6]-[9]. Ultimately, all such prior analysis techniques tend to be ad-hoc and a more systematic approach is desired.

This paper highlights an alternative method of analysis that uses the theory of conversion matrices. Conversion matrices have been extensively studied in literature in the area of computer simulation of complex time-varying circuits [12], and its use has even been extended to non-linear circuits [13], [14]. This paper provides a brief overview of the formulation of such an analysis. The approach is then applied to a mixer-first receiver, which is a common LPTV circuit, and basic results have been reproduced to show its accuracy. Further, some new results that were not obtained in prior art have also been derived.

II. Conversion Matrices

Let us define the frequency vector of a frequency transform of a signal $x(t)$ in an LPTV system as the vector $\underline{X}(\omega) = \begin{bmatrix} X(\omega - K\omega_p) & X(\omega - (K-1)\omega_p) & \cdots & X(\omega + K\omega_p) \end{bmatrix}^T$ for $\omega \epsilon \left(-\frac{\omega_p}{2}, \frac{\omega_p}{2}\right]$, where $X(\omega)$ is the Fourier transform of $x(t)$, $T_p = 2\pi/\omega_p$ is the fundamental period of the system, and $K \to \infty$ is a large positive integer. Then defining $\underline{U}(\omega)$ and $\underline{Y}(\omega)$ for the input and output of the system respectively, and using (1) with the summation index m running from $-K$ to K, it can be shown that $\underline{Y}(\omega) = \mathbb{H}(\omega)\underline{U}(\omega)$, where $\mathbb{H}(\omega) =$

$$\begin{bmatrix} H_0(\omega - K\omega_p) & \cdots & H_{-K}(\omega - K\omega_p) & \cdots & H_{-2K}(\omega - K\omega_p) \\ \vdots & \cdots & \vdots & \cdots & \vdots \\ H_K(\omega) & \cdots & H_0(\omega) & \cdots & H_{-K}(\omega) \\ \vdots & \cdots & \vdots & \cdots & \vdots \\ H_{2K}(\omega + K\omega_p) & \cdots & H_K(\omega + K\omega_p) & \cdots & H_0(\omega + K\omega_p) \end{bmatrix} \tag{2}$$

is referred to as the conversion matrix (or the "*harmonic transfer matrix*" [11]) of the LPTV system.

By itself, (2) is just the matrix form of (1), and does not give any extra information. However, for simple switching components the HTFs, and hence $\mathbb{H}(\omega)$ can be easily derived [12]. For example, consider an LPTV capacitor, whose capacitance is varying as $C(t) = C(t + T_p)$. The voltage and the current across the capacitor are related in the time and frequency domains by the following relations:

$$i(t) = C(t)\frac{dV(t)}{dt} \xleftrightarrow{\mathcal{F}} I(\omega) = C(\omega) * j\omega V(\omega)\ , \tag{3}$$

where $*$ is the convolution operator. Since $C(t)$ is periodic, it can be expanded as a Fourier series and its Fourier transform, $C(\omega)$, can be shown to be a sum of impulses at $\omega = m\omega_p$ with amplitudes C_m, where m is an integer, and C_m is the coefficient of $e^{jm\omega_p t}$ in the Fourier series expansion of $C(t)$: $C(\omega) = \sum_{m=-\infty}^{\infty} C_m \delta(\omega - m\omega_p)$. Then (3) gives:

$$I(\omega) = \sum_{m=-\infty}^{\infty} j(\omega - m\omega_p) V(\omega - m\omega_p) C_m. \tag{4}$$

Defining vectors $\underline{V}(\omega)$ and $\underline{I}(\omega)$ as before, (4) can be written in matrix form as $\underline{I}(\omega) = j\mathbb{C}\mathbf{\Omega}(\omega)\underline{V}(\omega)$, where $\mathbf{\Omega}(\omega) = diag\ \{[\omega - K\omega_p \quad \cdots \quad \omega \quad \cdots \quad \omega + K\omega_p]\}$, and

$$\mathbb{C} = \begin{bmatrix} C_0 & C_{-1} & \cdots & C_{-2K} \\ C_1 & C_0 & \cdots & C_{-2K+1} \\ \vdots & \vdots & \vdots & \vdots \\ C_{2K} & C_{2K-1} & \cdots & C_0 \end{bmatrix}. \tag{5}$$

The relation thus obtained, $\underline{I}(\omega) = j\mathbb{C}\mathbf{\Omega}(\omega)\underline{V}(\omega)$, is remarkably similar to the Fourier domain relation for a constant capacitor , i.e., $I(\omega) = jC\omega V(\omega)$. Hence $\mathbb{Y}_C(\omega) = j\mathbb{C}\mathbf{\Omega}(\omega)$ can be called the conversion matrix of the *"LPTV admittance"* of the switching capacitor. This relation is invertible for well-behaved capacitor variations, i.e. the conversion matrix of the *"LPTV impedance"* can be obtained by inverting the matrix of the LPTV admittance and vice versa. Similar relations can be obtained for all other LPTV elements, a subset of which is reported in Table I. Note that matrices $\mathbb{R}$ and $\mathbb{L}$ have the same form as $\mathbb{C}$ in (5).

Table I
BASIC CONVERSION MATRIX RELATIONS

Component	LPTV Relation
Resistor	$\underline{V}(\omega) = \mathbb{R}\underline{I}(\omega)$
Capacitor	$\underline{I}(\omega) = j\mathbb{C}\mathbf{\Omega}(\omega)\underline{V}(\omega)$
Inductor	$\underline{V}(\omega) = j\mathbb{L}\mathbf{\Omega}(\omega)\underline{I}(\omega)$

The most important property of the frequency vectors is that they follow linearity. Hence, linear Kirchoff's law relations that hold for time-domain voltage and currrent signals hold for their corresponding frequency vectors. This implies that other well known LTI results, such as series and parallel combination of impedances, Thevenin and Norton equivalent circuits, etc., have their conversion matrix equivalents as well. Hence by using such circuit laws, and basic conversion matrices (such as those in Table I), arbitrary LPTV circuits can be analyzed to derive their conversion matrices. To illustrate, this technique is applied to the mixer-first receiver.

III. MIXER-FIRST RECEIVERS

Mixer-first receivers, such as the one whose schematic is shown in Fig. 1(a), are promising candidates for widely programmable RF receiver front-ends. Here, the RF input signal is downconverted by four switches that are controlled by clocks with 25% duty cycle with a period, T_p, as shown in the figure. The in-phase and quadrature-phase outputs are measured differentially between the nodes $V_{I+}(t)$ and $V_{I-}(t)$ and between the nodes $V_{Q+}(t)$ and $V_{Q-}(t)$ respectively. Its behavior can be readily analyzed using the proposed approach as shown below.

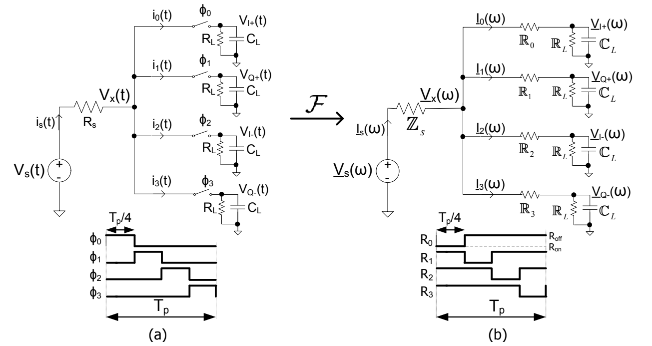

Figure 1. A mixer-first receiver

Let $\mathbb{R}_n$ denote the conversion matrix of the LPTV resistance of the switch in the n^{th} branch. The resultant Fourier domain equivalent circuit is shown in Fig. 1(b) wherein the relevant node voltages and branch currents are labeled. It can be readily shown that the differential in-phase output voltage (its frequency vector, actually) is given by:

$$\begin{aligned} \underline{V_I}(\omega) &= \mathbb{Z}_L \underline{I_0} - \mathbb{Z}_L \underline{I_2} \\ &= \mathbb{Z}_L \left[(\mathbb{R}_0 + \mathbb{Z}_L)^{-1} - (\mathbb{R}_2 + \mathbb{Z}_L)^{-1} \right] \underline{V_x}(\omega), \end{aligned} \tag{6}$$

where $\mathbb{Z}_L$ is the conversion matrix of the LPTV load impedance, i.e., $\mathbb{Z}_L = \left[R_L^{-1}\mathbb{I} + jC_L\mathbf{\Omega}(\omega) \right]^{-1}$, $\mathbb{I}$ being the identity matrix. Note that $\underline{V_x}$ can be obtained as a voltage divider between the LPTV source impedance, $\mathbb{Z}_s$, and the LPTV input impedance, $\mathbb{Z}_{in}$:

$$\underline{V_x}(\omega) = \mathbb{Z}_{in}(\omega) \left(\mathbb{Z}_s + \mathbb{Z}_{in}(\omega) \right)^{-1} \underline{V_s}(\omega), \tag{7}$$

where $\mathbb{Z}_s = R_s\mathbb{I}$. The conversion matrix of the LPTV input impedance can be shown, using series and parallel impedance combination rules, to be:

$$\mathbb{Z}_{in}(\omega) = \left(\sum_{n=0}^{3} \left[\mathbb{R}_n + \mathbb{Z}_L \right]^{-1} \right)^{-1}, \tag{8}$$

The conversion matrix of the receiver, $\mathbb{H}(\omega)$, defined as $\underline{V_I}(\omega) = \mathbb{H}(\omega)\underline{V_s}(\omega)$, can be derived simply by substituting (8) in (7), and the result in (6). A similar expression can be found for the differential quadrature-phase output voltage. The components of $\mathbb{H}(\omega)$ give the required HTFs as shown in (2).

These expressions can be evaluated given numerical circuit components, as illustrated below for an example mixer-first receiver. Note that prior art [4], [5], [10] has already analyzed this circuit, but assuming ideal clocks i.e., no duty cycle errors, instantaneous clock transitions etc., arguably to render analysis complexity manageable. However, considering clock non-idealities is very easy in the proposed technique: only the LPTV resistance matrices, $\mathbb{R}_n$, needs to be altered according to the actual resistance variation, but the expressions derived above remain the same. To illustrate, an example case of resistance variation due to non-zero clock transition widths is considered here, characterized by the parameter β, as shown in Fig. 2. The ideal case is represented by $\beta = 0$.

Assuming an OFF resistance, R_{off}, an ON resistance, R_{on}, $\mathbb{R}_n$ can be found from the corresponding periodic resistance

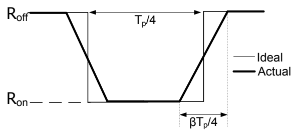

Figure 2. Non-ideal clock-edge model

variation, $R_n(t)$ (ideally varying as shown in Fig. 1(b)). Then the coefficient of $e^{jm\omega_p t}$ in the Fourier series of $R_n(t)$ can be found as $R_{n,m} = R_{n,m,ideal} + \triangle R_{n,m}$, where

$$\begin{aligned} R_{n,m,ideal} &= \tfrac{1}{m\pi}\left(R_{off} - R_{on}\right) sin\left(\tfrac{3m\pi}{4}\right) exp\left(-\tfrac{j\pi mn}{2}\right), \\ \Delta R_{n,m} &= \tfrac{1}{m\pi}\left(R_{off} - R_{on}\right) sin\left(\tfrac{m\pi}{4}\right) exp\left(-\tfrac{j\pi mn}{2}\right) \times \\ & \left[1 - \tfrac{4}{m\pi\beta} sin\left(\tfrac{m\pi\beta}{4}\right)\right], \end{aligned}$$

with $R_{n,0,ideal} = \frac{3}{4}(R_{off} - R_{on}) + R_{on}$, and $\Delta R_{n,0} = 0$. Note that the error term, $\triangle R_{n,m}$, appears due to non-zero β.

In the following, let $R_{off} = 10k\Omega$, $R_{on} = 0\Omega$, $R_s = 50\Omega$, $R_L = \frac{\pi^2}{2} R_s$ and switching frequency $\omega_p = 2\pi/T_p$ be such that $\omega_p/\omega_{RC} = 50$, where $\omega_{RC} = 1/R_s C_L$. A value of $K = 500$ was used in (2) for constructing all conversion matrices. For Cadence simulations, the switches were modeled as periodically varying resistors using Verilog-A.

A. Frequency Response

The frequency slice vector of the in-phase output, $\underline{V_I}(\omega)$, is calculated using (6)-(8), the slices combined to obtain $V_I(\omega)$ according to (3), and the magnitude of the result is plotted in Fig. 3. An input spanning the frequency slices centered around the fundamental switching frequency was used and ideal clock edges were assumed. Note that the downconverted output appears around DC and is shaped by the roll-off due to the capacitor at the output node, exactly as expected and predicted by prior art.

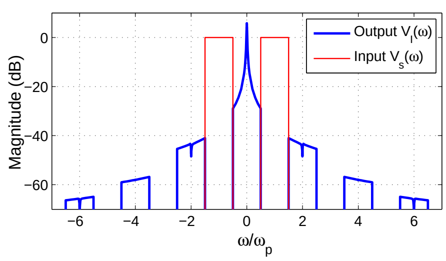

Figure 3. Receiver response to an input applied only in the frequency slices around $\pm\omega_p$

B. Downconversions

Mixer-first receivers are also known to downconvert frequency slices around odd harmonics of the switching frequency, $n\omega_p$, where n is an odd integer, to around DC. To confirm, the calculated magnitude of the function of HTFs, $H_n(\omega)+H_{-n}(\omega)$, which is the effective transfer function from the input frequency slices around $\pm n\omega_p$ to output's DC slice, is plotted in Fig. 4 for odd integers n for the ideal clock case i.e. $\beta = 0$. The plots are in good agreement with prior art.

The calculated effect of non-zero width clock transitions on the downconversion from $\pm\omega_p$ is plotted in Fig. 5 for two values of β. In the absence of prior art, the calculations are compared against Cadence SPECTRE PSS-PAC simulations, again showing excellent agreement.

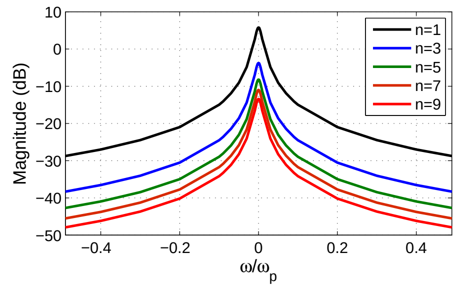

Figure 4. Receiver output around DC to an input applied only in the frequency slices around $\pm n\omega_p$ (as shown in Fig. 3)

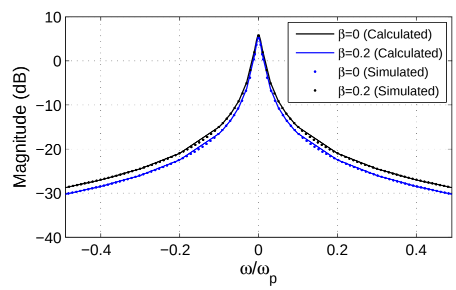

Figure 5. Receiver response around DC to an input applied only in the frequency slices around $\pm\omega_p$ in the case of imperfect clock edges

C. Noise Figure

Since the proposed technique calculates all HTFs, it is straightforward to calculate the noise figure degradation due to folding of noise from the source resistor. The noise figure (NF), considering up to M harmonics at an offset of ω from ω_p, is:

$$NF(\omega) = \frac{\sum_{n=-M}^{M} |H_n(\omega)|^2}{|H_1(\omega)|^2 + |H_{-1}(\omega)|^2}. \tag{9}$$

Considering $\beta = 0$, and up to 51 harmonics of the switching frequency, the calculated noise figure is $1.2272 = 0.889dB$, and is flat across the band as is expected for noise from source resistor, comparing very well with predictions from prior art.

D. Input Impedance

The input impedance offered by the receiver is important for proper matching at the RF interface, especially when driven directly by the antenna. We showed how the conversion matrix for the input impedance matrix, $\mathbb{Z}_{in}(\omega)$, could be easily calculated in (8). Its diagonal entries, i.e. $Z_{in,0}(\omega)$, give the input impedance. The calculated values around the switching frequency are plotted in Fig. 6 for the ideal case. At exactly the switching frequency, the calculated input impedance is purely real and near 50Ω. This is in excellent agreement with prior art, which predicts a value of $\frac{2}{\pi^2}R_L$ (50Ω in this example) for ideal clocks and ideal switches, i.e. $R_{on} = 0$ and $R_{off} \to \infty$.

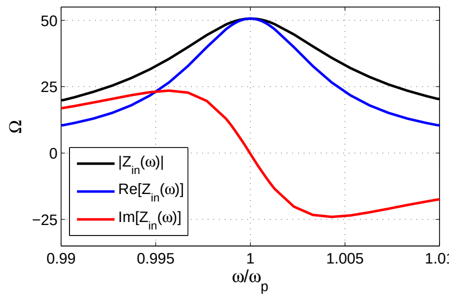

Figure 6. Receiver input impedance around the switching frequency, ω_p

Fig. 7 plots the calculated effect of non-zero clock transition times on the input impedance, and compares it with values simulated using Cadence SPECTRE PSS-PAC simulations. Note that even a small transition width (e.g., $\beta = 0.01$) causes about 20% higher input impedance. As mentioned before, prior art has been unable to predict this effect, highlighting the value of the proposed analysis technique.

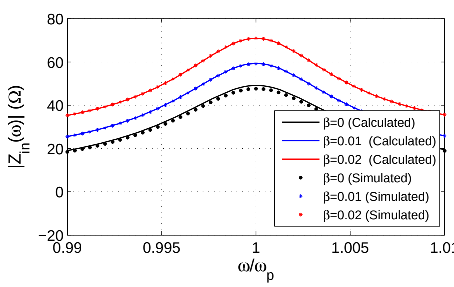

Figure 7. Receiver input impedance around the switching frequency, ω_p, in the case of imperfect clock edges

The effect of parasitic elements can also be easily included in the analysis. For example, suppose a parasitic capacitance, $C_p = \alpha C_L$, appears at the intermediate node, V_x, in Fig. 1(a), i.e. in parallel to receiver. To account for it, $\mathbb{Z}_{in}(\omega)$ in (7) just needs to be altered to:

$$\mathbb{Z}_{in}(\omega) = \left(\mathbb{Y}_p + \sum_{n=0}^{3} \left[\mathbb{R}_n + \mathbb{Z}_L \right]^{-1} \right)^{-1}, \tag{10}$$

where $\mathbb{Y}_p = jC_p\mathbf{\Omega}(\omega)$. With this modification, the effects of C_p can be easily studied. For example, the effect of C_p on the receiver input impedance around ω_p is shown in Fig. 8 , along with simulation results using Cadence SPECTRE PSS-PAC. Notice how a parasitic C_p of even 0.2% of the load capacitance, C_L, can reduce the input impedance by about 10%. A slight shift in the peak of the impedance curve can also be observed. Similarly, to consider a complex source impedance, only $\mathbb{Z}_s$ in (7) needs to be changed.

IV. Conclusions

In this paper, an analysis of a mixer-first receiver using conversion matrices is presented. The approach uses conversion matrices that allows LPTV circuits to be analyzed using familiar circuit theorems such as Kirchoff's laws, in a manner similar to LTI circuits. Important results found in prior art were reproduced to verify the analysis technique and the effects of a few, but important circuit non-idealities not considered in prior art were also calculated.

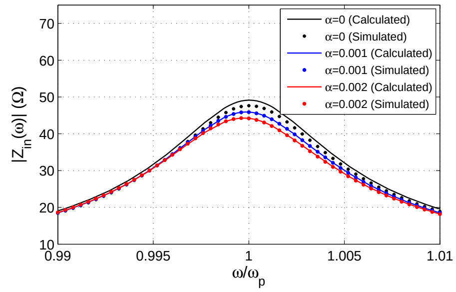

Figure 8. Receiver input impedance around the switching frequency, ω_p, with parasitic capacitance

References

[1] Nekovee, M., "Cognitive Radio Access to TV White Spaces: Spectrum Opportunities, Commercial Applications and Remaining Technology Challenges," *New Frontiers in Dynamic Spectrum, 2010 IEEE Symposium on* , vol., no., pp.1,10, 6-9 April 2010.

[2] Abidi, A.A., "The Path to the Software-Defined Radio Receiver," *Solid-State Circuits, IEEE Journal of* , vol.42, no.5, pp.954,966, May 2007.

[3] Zadeh, Lotfi A, "Frequency Analysis of Variable Networks," *Proceedings of the IRE* , vol.38, no.3, pp.291,299, March 1950.

[4] Mirzaei, A.; Darabi, H.; Leete, J.C.; Yuyu Chang, "Analysis and Optimization of Direct-Conversion Receivers With 25% Duty-Cycle Current-Driven Passive Mixers," *Circuits and Systems I: Regular Papers, IEEE Transactions on* , vol.57, no.9, pp.2353,2366, Sept. 2010.

[5] Mirzaei, A.; Darabi, H., "Analysis of Imperfections on Performance of 4-Phase Passive-Mixer-Based High-Q Bandpass Filters in SAW-Less Receivers," *Circuits and Systems I: Regular Papers, IEEE Transactions on* , vol.58, no.5, pp.879,892, May 2011.

[6] Yuh Sun; Frisch, I.T., "A General Theory of Commutated Networks," *Circuit Theory, IEEE Transactions on* , vol.16, no.4, pp.502,508, Nov 1969.

[7] Strom, T.; Signell, S., "Analysis of periodically switched linear circuits," *Circuits and Systems, IEEE Transactions on* , vol.24, no.10, pp.531,541, Oct 1977.

[8] Soer, M. C M; Klumperink, E.A.M.; de Boer, P.-T.; van Vliet, F.E.; Nauta, B., "Unified Frequency-Domain Analysis of Switched-Series- RC Passive Mixers and Samplers," *Circuits and Systems I: Regular Papers, IEEE Transactions on* , vol.57, no.10, pp.2618,2631, Oct. 2010.

[9] Ghaffari, A.; Klumperink, E.A.M.; Soer, M. C M; Nauta, B., "Tunable High-Q N-Path Band-Pass Filters: Modeling and Verification," *Solid-State Circuits, IEEE Journal of* , vol.46, no.5, pp.998,1010, May 2011.

[10] Andrews, C.; Molnar, A.C., "Implications of Passive Mixer Transparency for Impedance Matching and Noise Figure in Passive Mixer-First Receivers," *Circuits and Systems I: Regular Papers, IEEE Transactions on* , vol.57, no.12, pp.3092,3103, Dec. 2010.

[11] Vanassche, P.; Gielen, G.; Sansen, Willy, "Symbolic modeling of periodically time-varying systems using harmonic transfer matrices," *Computer-Aided Design of Integrated Circuits and Systems, IEEE Transactions on* , vol.21, no.9, pp.1011,1024, Sep 2002.

[12] S. A. Maas, *Nonlinear microwave and RF circuits*, 2nd Ed., Artech House, 2003.

[13] Chua, L.O.; Ng, C.Y., "Frequency-domain analysis of nonlinear systems: formulation of transfer functions," *Electronic Circuits and Systems, IEE Journal on* , vol.3, no.6, pp.257,269, November 1979.

[14] Kundert, K.S.; Sangiovanni-Vincentelli, A, "Simulation of Nonlinear Circuits in the Frequency Domain," *Computer-Aided Design of Integrated Circuits and Systems, IEEE Transactions on* , vol.5, no.4, pp.521,535, October 1986.